Reentrant melting of lanes of rough circular disks

Md. Samsuzzaman[*] and Ahmed Sayeed[†]

Department of Physics, Savitribai Phule Pune University, Pune 411007, India

Arnab Saha ⬤[‡]

Department of Physics, University Of Calcutta, 92 Acharya Prafulla Chandra Road, Kolkata-700009, India

We consider binary suspension of rough, circular particles in two dimensions under athermal conditions. The suspension is subject to a time-independent external drive in response to which half of the particles are pulled along the field direction, whereas the other half is pushed in the opposite direction. Simulating the system with different magnitude of external drive in steady state, we obtain oppositely moving macroscopic lanes only for a moderate range of external drive. Below as well as above the range we obtain states with no lane. Hence we find that the no-lane state reenters along the axis of the external drive in the nonequilibrium phase diagram corresponding to the laning transition, with varying roughness of individual particles and external drive. Interparticle friction (contact dissipation) due to the roughness of the individual particle is the main player behind the reentrance of the no-lane state at high external drives.

I. INTRODUCTION

The relation between the microscopic processes and the macroscopic behavior of a system is pertinent to many scientific discourses. Lane formation is a nonequilibrium self-organization process observed in various binary mixtures of two oppositely moving species. Under certain conditions, the microscopic elements of these two species segregate from a homogeneously mixed state to form oppositely moving macroscopic lanes composed of different species. This dynamical transition occurs at widely varying time and length scales starting from pedestrian dynamics [1,2] and army ants [3] all the way to collective cell dynamics [4–6], driven binary plasma [7,8], granular flows [9–11], and driven colloids [12–14].

Colloids, when driven far from thermal equilibrium, exhibit diverse spatiotemporal patterns and novel transport properties due to intricate self-organization processes [15,16]. One such prototype of nonequilibrium phenomenon in driven binary colloids is lane formation. It has been studied extensively in theory [17–23] and in experiments [12–14]. In this particular problem a homogeneously mixed binary colloid is considered where the constituent colloidal particles of different species move in opposite directions in response to an external drive. It has been shown that depending on various parameters of the system (e.g., average density, the strength of external drive, and temperature), oppositely moving lanes, composed of the particles of different species present in the suspension, can emerge from a homogeneously mixed state

both by constant (i.e., time-independent) [12,13] as well as time-periodic (e.g., ac drive) external drive [14]. The colloidal lanes can appear perpendicular [14] as well as parallel [13] to the external drive. In the case of the lane formation parallel to the external drive, the transition occurs when the magnitude of the external driving force exceeds a finite threshold value [17]. As the lane forms, it has been shown that the correlation decays algebraically parallel to the drive and exponentially perpendicular to the drive [24]. The transition is first order [17] and has considerable finite-size effects [25]. For example, in a finite system, the transition is quite sharp. In the thermodynamic limit when the system size diverges, the correlation along the external drive does not. It signifies a smooth crossover in this limit [25]. Another major finding is the reentrance of a no-lane state with increasing density and keeping other parameters (e.g., external force) fixed. For a fixed driving force (high enough to form lanes) with increasing particle density, first there occurs a transition from the no-lane state toward the laned state which is followed by a second transition which brings the no-lane state back as the particles get jammed at high densities [26].

Recently it has been realized that microscopic frictional contacts among the colloidal particles induced by surface roughness of the particles can produce novel macroscopic effects (e.g., Ref. [27]). An important example of such tribological effect is discontinuous shear thickening (DST) [28–35] where effective viscosity of the suspension increases abruptly by several orders of magnitude (i.e., much stronger dependence than Bagnold scaling [36]) with increasing shear rate close to its critical value. DST is exhibited in a variety of suspensions with Brownian [37–48] as well as non-Brownian [33,44,49–57] characters suggesting DST as a universal behavior of dense suspensions where thermal motion of the particles does not seem to contribute significantly (e.g.,

---

[*]samsuzz@gmail.com
[†]ahmedsayeediisc@gmail.com
[‡]sahaarn@gmail.com

Ref. [56]). Indeed, DST occurs in experiments with rigid non-Brownian neutrally buoyant particles suspended in a Newtonian fluid in the Stokes regime [33,53]. Here we also note that depending on the density and surface roughness of the particles, the interparticle friction can also be pivotal in the collective dynamics of *active granular* systems [58,59]. Few examples of such systems are sedimenting starch-rich grains—statoliths—in gravisensing plant cells [58] or synthetically prepared micromachined polar disks subjected to vertical vibration [60], where thermal fluctuations are subservient in comparison to the other forces including the active force present in the system. The underlying physics of such systems can also be applied to explore active systems in daily life, such as pedestrian dynamics or the dynamics of army ants.

Being motivated by above findings, we will explore here how the lane formation appears in the presence of interparticle friction under athermal conditions. In order to introduce dissipative interparticle force we will adapt a simple route introduced to model mechanics of foam [61]. Later it became useful to explore other related problems: shear thinning in adhesive dispersions [62]; dissipation and rheology of soft-core disks under shear [63]; plasticity in sheared glass [64]; avalanche-size distribution in a sheared amorphous solid under athermal condition [56,65]; influence of attractive interaction in granular suspensions [66]; jamming in confined, soft particles under gravity [67]; effective temperature in driven systems [68], etc. Essentially it assumes that the interparticle dissipative force that drags a particle is proportional to the velocity of the particle relative to the velocities of its nearest neighbors which are in contact to the particle. In the presence of such interparticle friction, here we will show that for a fixed density, in two dimensions, under athermal conditions, the lanes, which are formed as the external drive exceeds a threshold value (as also shown by the earlier studies on colloidal lane formation [17]), will become unstable if the external drive is increased further. In other words, with finite interparticle friction, at fixed average density but with increasing strength of external drive, there will be a reentrance of a no-lane state. Here we emphasize that the reentrance of the no-lane state obtained here differs fundamentally from the colloidal reentrance obtained earlier in Ref. [26] as it was obtained at fixed external drive and with increasing average density of the system where jamming played a crucial role.

We find that density plays an important role in laning of the particles with frictional contacts. Frictional contact between the particles increases with increasing density. Therefore, the interparticle friction induced by the contacts will be effective at higher densities. The average interparticle frictional force indeed decreases as the density of the system is reduced (see later). Hence it is enticing to conclude that lowering the density from a state with high external drive and high-enough density (at which the laned state is unstable due to the particle-scale roughness) may help to stabilize the laned state. Though it is important to note that for a laned state with fixed external drive, irrespective of the particle-scale roughness, lowering the density of the system causes the drop of the quality of the lanes and below a threshold value of the density, lanes disappear [26]. Therefore, if density is reduced, then interparticle

friction decreases but the quality of lanes also drops. Later in this paper we will discuss this in greater detail.

Next we will systematically detail our findings, starting from model description and then by describing and analyzing the results obtained by simulating the model. We investigate the laning transition by varying the external drive and interparticle friction keeping the average density of the system fixed (at a value suitable for laning) as well as by varying the density keeping the interparticle friction fixed. We also present an intuitive phenomenological toy model which produces results qualitatively similar to the simulation results.

II. MODEL

We consider a binary suspension of "a"- and "b"-type particles in two dimensions where each of the components has N_a and N_b particles within area A. The average density of the system $\rho = (N_a + N_b)/A$. The average densities of each of the components are $\rho_a = N_a/A$ and $\rho_b = N_b/A$. Here we consider the 1:1 mixture where $N_a = N_b = N$.

The particles are interacting with each other via a conservative force derived from an effective pair potential U that depends on the distance between the particles of the concerned pair. For simplicity we consider the symmetric case where $U_{aa} = U_{bb} = U_{ab} = U$. The interparticle interaction that we consider here is screened Coulomb interaction [17],

$$U(r_{ij}) = V_0 \frac{\exp[-\kappa(r_{ij} - \sigma)]}{(r_{ij}/\sigma)}. \tag{1}$$

Here r_{ij} is the distance between a pair of the particles denoted by the indices i and j, V_0 is the energy scale, and σ is the particle diameter that sets a length scale. The inverse screening length $\kappa = 4\sigma$ governs the range of the interaction. This interaction is used to model charge-stabilized suspensions where κ is the range of the interaction which can be tuned, for example, chemically [69].

Apart from the conservative interparticle forces, the particles are also going through dissipative forces. One of them is originated from the frictional drag force $\mathbf{F}_i^p$ due to the surrounding fluid. It is proportional to velocity $\mathbf{v}_i$ of the ith particle, i.e., $\mathbf{F}_i^p = -\gamma \mathbf{v}_i$ where γ is the friction coefficient between the particle and the fluid that depends on the viscosity η of the surrounding fluid [70]. Here we assume that the effect of hydrodynamic interaction among the suspended particles are negligibly small which can be due to screening [71].

Another source of dissipative force that an individual particle can face, is from interparticle friction. It is a short-ranged dissipative force that depends on the average relative velocity between a particle and its nearest neighbors which are in contact [56,63,65,68], i.e., $\mathbf{F}_i^q = -\frac{\mu}{N_i} \sum_j H(u_{ij})(\mathbf{v}_i - \mathbf{v}_j)$ where $H(u_{ij}) = 1$ if $u_{ij} = \sigma - r_{ij} \geqslant 0$ and $H(u_{ij}) = 0$ otherwise. Here N_i is the number of nearest neighbors of ith particle for which $H = 1$. If $N_i = 0$, as there is no neighboring particle, $\mathbf{F}_i^q = 0$.

Finally, the particles are also experiencing constant external field along a particular direction (here without loosing any generality we choose the direction to be $\hat{\mathbf{x}}$). Type "a" particles are driven along $+\hat{\mathbf{x}}$ and "b"-type particles are driven in the opposite direction due to the external force $\mathbf{F}_{\text{ext}} = F_{\text{ext}}\hat{\mathbf{x}}_i$. Clearly, the two types of particles ("a" and "b") are solely

distinguished by their response to the external field. Therefore the equation of motion of the particles with unit mass is given by $\frac{d^2\mathbf{r}_i}{dt^2} = \mathbf{F}_i^p + \mathbf{F}_i^q - \sum_j \mathbf{\nabla}_i U \pm \mathbf{F}_{\text{ext}}$ where the positive sign is used for "a"-type particles and negative sign is used for "b"-type particles. We consider that the thermal fluctuations are negligibly small in comparison to the other forces present in the system.

We consider σ to be the unit for length and $1/\gamma$ to be the unit for time. With these units the left-hand side of the equation of motion mentioned before becomes $\gamma^2\sigma\frac{d^2\tilde{\mathbf{r}}_i}{d\tilde{t}^2}$ where $\tilde{\mathbf{r}}_i$ is dimensionless position vector of the particle at dimensionless time $\tilde{t}$. With these units the frictional drag from fluid becomes $\gamma^2\sigma\tilde{\mathbf{F}}_i^p$ where $\tilde{\mathbf{F}}_i^p$ is the dimensionless velocity of the ith particle. Similarly, interparticle friction becomes $\mu\gamma\sigma\tilde{\mathbf{F}}_i^q = \alpha\gamma^2\sigma\tilde{\mathbf{F}}_i^q$ where $\mu/\gamma = \alpha$ and $\tilde{\mathbf{F}}_i^q$ is the dimensionless relative velocity between a particle and its nearest neighbors which are in contact. By dividing the both sides of the equation of motion (mentioned earlier) with $\gamma^2\sigma$ and introducing dimensionless gradient operator as $\frac{1}{\sigma}\tilde{\mathbf{\nabla}}_i$ we obtain a dimensionless interparticle energy scale as $U_0 = V_0/\gamma^2\sigma^2$. Similarly, we obtain a nondimensionalized magnitude of the externally applied driving force as $\tilde{F}_{\text{ext}} = F_{\text{ext}}/\gamma^2\sigma$. Therefore the equation of motion with dimensionless quantities reads

$$\frac{d^2\tilde{\mathbf{r}}_i}{d\tilde{t}^2} = \tilde{\mathbf{F}}_i^p + \alpha\tilde{\mathbf{F}}_i^q - \sum_j \tilde{\mathbf{\nabla}}_i \tilde{U} \pm \tilde{\mathbf{F}}_{\text{ext}}, \qquad (2)$$

where $\tilde{U} = U_0\frac{\exp(-\kappa\sigma(\tilde{r}_{ij}-1))}{\tilde{r}_{ij}}$, $\tilde{r}_{ij} = r_{ij}/\sigma$. The average dimensionless density is given by $\tilde{\rho} = \rho\sigma^2$. For brevity of notation, from now on we will omit tilde from the dimensionless variables.

III. SIMULATION METHOD

We have carried out simulation by numerically integrating the equation of motion given in Eq. (2). For the simulations, unless stated otherwise, the initial state is a homogeneously mixed, nonlaned state on which $\pm\mathbf{F}_{\text{ext}}$ is applied. After driving the system with the external drive for long, the system reaches at a nonequilibrium steady state where we collect the data (position and velocities of the particles) to analyze. Depending on the values of the relevant parameters (e.g., ρ, F_{ext}, and α), lanes may or may not emerge in the steady state.

Initially, the positions and velocities of the particles are distributed randomly. Once $\mathbf{F}_{\text{ext}}$ is switched on, the initial positions of N_a and N_b particles are chosen randomly from $2N$ particles such that the initial configurations represent a well-mixed binary mixture of "a"- and "b"-type particles. To update the positions and velocities of the particles we use the velocity verlet algorithm [72] with time discretization $\delta t = 0.0001$ for a total simulation run of 6×10^7 time steps. Positions and velocities of the particles are recorded when the system reaches a nonequilibrium steady state after 50×10^4 steps, when the average lane order parameter of the system does not alter significantly over time. The results presented here are averaged over time in nonequilibrium steady states and also over five different realizations. For all our simulations we have kept the values of N, γ, V_0, and σ constant. We vary

F_{ext}, ρ, and α to explore their effect on laning. We keep ρ fixed while varying (F_{ext}, α) and α fixed while varying (F_{ext}, ρ).

The data presented here are obtained by simulating 2000 particles confined within a square box with periodic boundary condition in both the x and y directions. When we explore the effect of varying F_{ext} and α, the area is fixed at $A = 44\sigma \times 44\sigma$ to keep the average density fixed around 1 which is suitable for the lane formation provided the external driving force exceeds a threshold value [17,26]. While exploring the effect of average density on laning, we vary the average density by varying the area of the simulation box, keeping the number of the particles fixed.

IV. RESULTS

A. Lane order parameter and nonuniformity of the density profile

We begin by analyzing the nonequilibrium steady states of the system obtained by varying F_{ext} and α at fixed ρ. Later, under Discussion, we will detail the effect of varying average density on laning. The states are characterized by the spatial organization as well as the dynamical properties of the system. Below we will develop the tools to characterize the steady states.

In a similar setup with colloidal binary suspensions, it is known that the system phase separates at finite temperature and the components move in opposite directions, forming oppositely moving parallel lanes [17]. The transition from no-lane state to laned state in colloidal binary suspension starts to occur after a finite threshold of external driving force. The transition is reversible and exhibits significant hysteresis. It is classified as a first-order nonequilibrium phase transition [17]. Note that there are fundamental differences between the system that we are concerned here and the system discussed in Ref. [17]: the present model includes interparticle contact dissipation and it does not involve thermal fluctuations which are relevant for non-Brownian suspensions (e.g., Ref. [68]). Our aim here is to explore the consequence of interparticle friction on lane formation in two dimensions when the thermal fluctuation is negligibly small. To characterize the spatial organization of the particle in the context of lane formation, we borrow the lane order parameter from Ref. [17]. We define the lane order parameter by assigning every particle a quantity ϕ_i as

$$\phi_i = 1 \quad \text{when } |y_j - y_i| > \rho^{-1/2}/2$$
$$= 0 \quad \text{elsewhere}, \qquad (3)$$

where i and j indicate "a"-type and "b"-type particles, respectively. This can be termed as local (i.e., defined for individual particle at time t) lane order parameter. We define the global (i.e., defined for the whole system at a given configuration at time t) lane order parameter as

$$\phi = \frac{1}{N}\sum_i \phi_i, \qquad (4)$$

which can then be averaged over time and realizations in steady states. Note that for a perfectly mixed, nonlaned state ϕ is zero. It increases from zero when the lanes start to appear. For a perfectly laned state ϕ is unity.

We will see later that with increasing F_{ext}, after a certain threshold value (say, F_c), particles phase separate forming oppositely moving lanes. This phenomena is similar to the binary colloidal suspension as in Ref. [17]. If F_{ext} is increased further, then the laned state continues up to a second threshold value of F_{ext} (say, F_c'). When F_{ext} is increased beyond F_c', irrespective of their type, particles tend to accumulate randomly creating high- as well as low-density regions. Hence the density profile of the system tends to be increasingly nonuniform with increasing F_{ext}. Eventually the lane structure is broken at high-enough $F_{\text{ext}} > F_c'$ and we obtain the reentrance of nonlaned state, which is the central theme of the present work. Therefore it is important to quantify the nonuniformity of the density distribution of the system. We will quantify the nonuniformity by calculating the standard deviation of the local density profile $g(x, y)$ of the system. Here $g(x, y)$ is the local probability density of finding a particle (irrespective of its type) between x to $x + dx$ and y to $y + dy$. Clearly $\int g(x, y)dxdy = 2N$. Computationally g is obtained by dividing the system into a grid of cells and then by counting the number of particles in each cell. For a given configuration the standard deviation is given in Eq. (5) where the angular bracket represents averaging over all the cells. It is noteworthy that the cell should not be very large as it becomes incapable to capture the nonuniformity of the density profile (extreme case: For the cell which is of the same size as the system, Σ vanishes). It should not be very small as well, i.e., it should be larger than the size of a single particle. The cell size we choose here is $4\sigma^2$. The results obtained by choosing different cell sizes (considerably far from extreme cases) are qualitatively the same. We report Σ after taking the averages over time and realizations in steady states,

$$\Sigma = \frac{\sqrt{\langle (g(x, y) - \rho)^2 \rangle}}{\rho}. \tag{5}$$

We emphasize that the types of the particles are not considered while calculating $g(x, y)$. Hence, for the states with uniform distribution of particles, irrespective of whether they contain lanes or not, Σ is very low. In other words, for states with uniform particle distribution, by measuring Σ one cannot distinguish between laned and nonlaned states. Σ increases when particles, disregarding their types, get accumulated in random places of the system, making the density profile nonuniform. Thus Σ is a measure of the nonuniformity in the position distribution of the particles.

The variation of ϕ and Σ with external force for different α is plotted in Fig. 1. From the plots it is evident that with $\alpha > 0$, ϕ has nonmonotonic dependence on F_{ext}. Initially, when $F_{\text{ext}} = 0$, the "a"- and "b"-type particles are homogeneously mixed with each other and therefore it is a no-laned state with $\phi = 0$. It increases with increasing F_{ext} and reaches at a plateau when F_{ext} goes beyond the threshold F_c. In this plateau region, even if F_{ext} increases, ϕ does not change considerably. This plateau continues until F_{ext} reaches at a second threshold value F_c'. When $F_{\text{ext}} > F_c'$, ϕ starts to decrease considerably with increasing F_{ext}. Hence the nonlaned state reenters. To distinguish between laned and no-lane state we consider a threshold $\phi_c = 0.75$ such that for laned states $\phi > \phi_c$ and for no-lane states $\phi < \phi_c$. We note from the figure that for $\alpha = 0$,
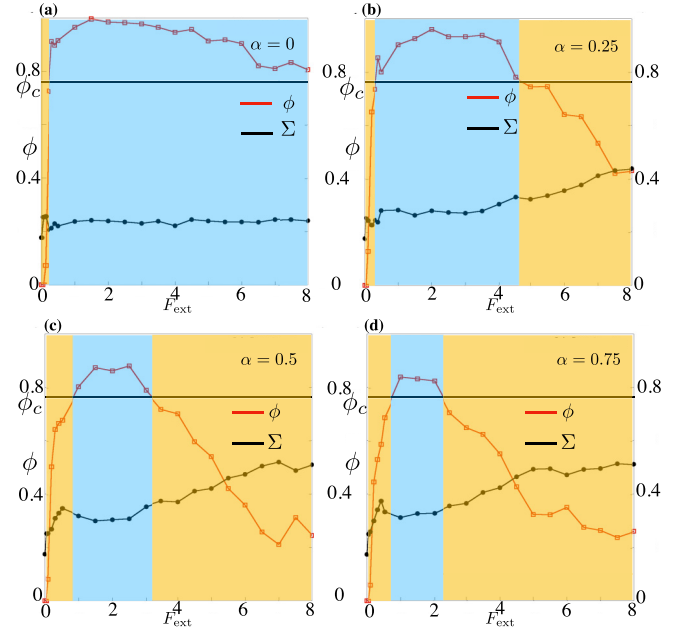

FIG. 1. Lane order parameter ϕ and standard deviation Σ of the density profile are plotted with external drive F_{ext} for $\alpha = 0, 0.25, 0.5, 0.75$ in (a), (b), (c), and (d), respectively. ϕ is in red and Σ is in black. The threshold of the lane order ϕ_c is shown by the horizontal straight line $\phi = \phi_c = 0.75$. The width of the blue region depicts the window $\Delta F = F_c' - F_c$ within which $\phi > \phi_c$, i.e., quality lanes occur in the system. The yellow region is where $\phi < \phi_c$. $F_{\text{ext}} = F_c$ is the left boundary of the blue region, which is the first threshold value of F_{ext} beyond which quality lanes form in steady states and therefore ϕ becomes larger than ϕ_c. With finite interparticle friction (i.e., $\alpha > 0$), $F_{\text{ext}} = F_c'$ is the right boundary of the blue region, which is the second threshold value of F_{ext} beyond which, lane quality drops and ϕ becomes smaller than ϕ_c. Clearly, without interparticle friction (i.e., for $\alpha = 0$), once the lanes are formed their quality does not drop considerably with increasing F_{ext} and therefore ϕ is larger than ϕ_c for all values of F_{ext} considered here. It is apparent from panels (b)–(d) that for $\alpha > 0$, Σ increases with F_{ext}, affecting the lane-quality. Hence ϕ drops below ϕ_c when $F_{\text{ext}} > F_c'$. Hence the no-lane state, which was there for $F_{\text{ext}} < F_c$, reenters when $F_{\text{ext}} > F_c'$.

$\phi > \phi_c \forall F_{\text{ext}} > F_c$ which is the reminiscent of lane formation in binary colloidal suspensions as explored in Ref. [17]. For $\alpha > 0$, due to the reentrance of the no-lane state, $\phi > \phi_c$ for $F_c < F_{\text{ext}} < F_c'$. Beyond this window of external drives $\Delta F = F_c' - F_c$, $\phi < \phi_c$. It is evident from the figure that ΔF decreases as α increases. Later we will be back to this point while estimating the threshold forces theoretically. In contrast to ϕ, when $\alpha = 0$, Σ does not change considerably with F_{ext}. This implies that though the particles of different species segregate to form lanes, irrespective of their species, they are uniformly distributed through out the system. On the other hand, when $\alpha > 0$, in contrast to ϕ, Σ increases monotonically with F_{ext}. This signifies that in presence of interparticle friction, with increasing F_{ext}, the density profile becomes increasingly nonuniform. Though for lower external drives ($F_c < F_{\text{ext}} < F_c'$) this nonuniformity is not so detrimental to the lane structure of the system such that it falls apart but at higher external forces ($F_{\text{ext}} > F_c'$) it is. Hence, with $\alpha > 0$,
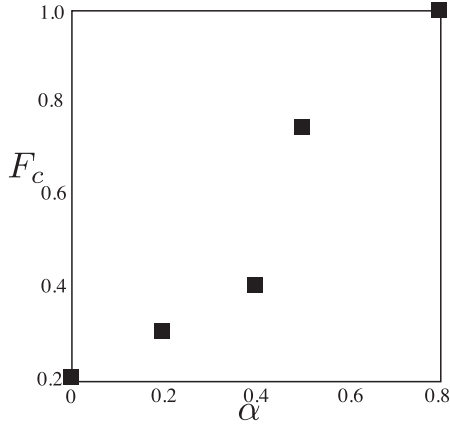
FIG. 2. Here F_c, i.e., the threshold values of F_{ext} required to form lanes are plotted for different values of the roughness parameter α. It shows that as the individual particles become more rough, larger external forces are required for lanes to emerge from a homogeneously mixed binary suspension.

at high external drives, ϕ drops below ϕ_c and one gets the no-lane state back.

It should be mentioned here that the no-lane states obtained for low external drive (i.e., $F_{ext} < F_c$) are more uniform than the no-lane states obtained at large external drives (i.e., $F_{ext} > F_c'$), which is the fundamental difference between them. It is reflected in the configurations given in Fig. 3 as well as from the plot of Σ with increasing F_{ext} in Fig. 1. Another important observation is that F_c increases as α increases. It is apparent from Fig. 2 where we have plotted F_c with different values of roughness parameter α. It implies that as the surface of the individual particles becomes more rough, stronger external drive is required to form lanes. Later we discuss this point again while estimating the threshold forces theoretically. Next we discuss the phase diagram of the laning transition with respect to the roughness parameter α and the magnitude of the external drive F_{ext}, at fixed density.

B. Phase diagram

The reentrant transition between laned and no-lane phases of the system is represented by the phase diagram in the α-F_{ext} plane in Fig. 3. With the heat map of ϕ and the broken lines as a guide to the eye in the α-F_{ext} plane we represent the phases.

For $\alpha = 0$ and very low F_{ext} ($0 < F_{ext} < 0.2$) no significant laning is observed ($\phi < \phi_c$). As F_{ext} increases and crosses the threshold F_c, system enters into the laned state ($\phi > \phi_c$) and it remains in the laned state for all values of F_{ext}. There is no signature of reentrance of the no-lane state with increasing F_{ext} when $\alpha = 0$. This is also true as far as α remains small ($\alpha \lesssim 0.15$). Thus, a minimum external drive is required to segregate the particles into distinct lanes which can be inferred from the fact that the external drive has to be larger than the other forces between any two pair of the particles moving opposite to each other.

The scenario changes drastically as α increases beyond 0.15 and the change is apparent for high F_{ext}. In this regime of α, as earlier, we observe that lanes appear into the system only when $F_{ext} > F_c$. F_c increases as we increase α. This implies
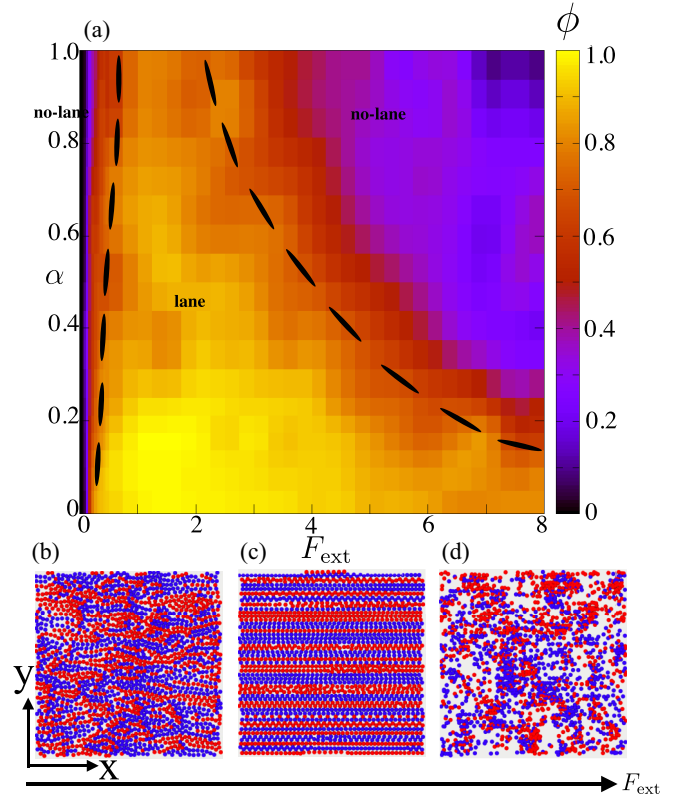

FIG. 3. (a) The heat map of the lane order parameter ϕ in the F_{ext}-α plane. It indicates that with finite interparticle friction ($\alpha > 0$), for very low and high F_{ext}, the system does not support any lane structure, whereas it is supported by the optimum values of F_{ext}, which occurs in between. Broken lines are drawn schematically as a guide to the eye to indicate the laned and no-lane phases. The phase diagram is constructed with a total of 22 different values of F_{ext} and 20 different α. [(b)–(d)] Typical configurations with increasing magnitude of external drive F_{ext}, shown by the long black arrow at the bottom. Red and blue colors of the particles indicate particles moving in the $+\hat{\mathbf{x}}$ and $-\hat{\mathbf{x}}$ directions, respectively.

that as the contact dissipation between the particles increases we need higher external drive to move them against each other to form lane. This is manifested in Fig. 2. In the context of lane formation, the qualitative difference between the particles with and without roughness appears as we increase F_{ext} further. We observe that when F_{ext} goes beyond a second threshold F_c', the lane quality falls. ϕ becomes smaller than ϕ_c. No-lane state reenters. Thus, in the α-F_{ext} plane, along the axis of increasing F_{ext}, first we have a region of no lanes, then a region of lanes, and finally another region of no-lane. This is the central result of our paper, which highlights the fact that it is not possible to have good lanes even if we increase the external drive to very high values in the presence of interparticle friction. We also observe that though F_c increases slightly but F_c' reduces considerably with increasing α. Hence the window ΔF, responsible for laning, shrinks with increasing α.

The typical configurations with increasing F_{ext} are shown in Figs. 3(b)–3(d). They demonstrate that for very low external drive, in steady state, lanes are not developed within the system [Fig. 3(b)]. It is developed only after crossing the finite

threshold value of the drive F_c. A typical laned configuration is shown in Fig. 3(c). When the external drive is increased further and eventually $F_{ext} > F_c'$, the lanes are broken due to interparticle friction and no-lane state reenters. The typical steady-state configuration in this regime is given in Fig. 3(d). It has been mentioned in the previous section that the no-lane state obtained for $F_{ext} < F_c$ is quite different from the no-lane state obtained $F_{ext} > F_c'$ and the difference is manifested by Σ.

C. Dynamical property

The transport along the direction of the external field is affected due to the interparticle friction. Lanes help transport. With finite interparticle friction the lane order is reduced at high external drive. Hence it is intuitive that the transport along the external drive will be affected as we increase the field. We quantify the transport along the direction of the external field by computing the drift velocity along the field in steady state. The drift velocity is defined as [17]

$$v_D^2 = \lim_{t \to \infty} \frac{\langle (x_i(t) - x_i(0))^2 \rangle}{t^2}, \qquad (6)$$

where $x_i(t)$ is the x position of ith particle of the system. We measure v_D after the system reaches at a steady state where ϕ fluctuates around a constant mean. The angular bracket indicates averaging over all particles (irrespective of their type) and then taking the average over time and realizations in steady states. We observe that as expected, drift velocity along the direction of the external field is reduced with increasing interparticle friction (Fig. 4). This has also become apparent from the inset of Fig. 4 that the rate of change of v_D with respect to F_{ext} (obtained from the slope of the straight line fitted with v_D vs. F_{ext} graph) decreases with α.

V. DISCUSSION

A. Interplay of F_{ext} and α at constant ρ

So far we have shown that with increasing external drive, not only the transition from a no-lane state to a laned state occurs in a driven binary suspension of oppositely moving rough particles under athermal conditions but a transition in reverse direction (laned to no-lane state) also occurs when the external drive is large enough. This reentrant transition occurs when the interparticle friction due to the roughness of the particles, affects their dynamics significantly. We have also shown that with increasing external drive, the density profile of the rough ($\alpha > 0$) particles become gradually nonuniform. Hence the well-formed lanes start to break at high external drives. Here we will discuss how these two transitions (no-laned state to laned state and the opposite) occurs.

We consider a state of the system of rough particles with $F_{ext} < F_c$. The system is in mixed, i.e., no-laned state. As the external drive is along $\hat{x}$, $\langle v_i^x \rangle \neq 0$, whereas $\langle v_i^y \rangle = 0$. The average velocity of the neighbours of the ith particle in both the directions is zero as it is a mixed state. Therefore, from the equation of motion, at high damping, the predominant contribution to the average velocity of the ith particle along $\hat{x}$, is from the external drive, which is $u_1 \equiv \frac{F_{ext}}{\gamma + \mu}$, whereas along $\hat{y}$ it is $u_2 \equiv \frac{V_0}{\sigma \gamma}$. The lanes start to form when $u_1 > u_2$.
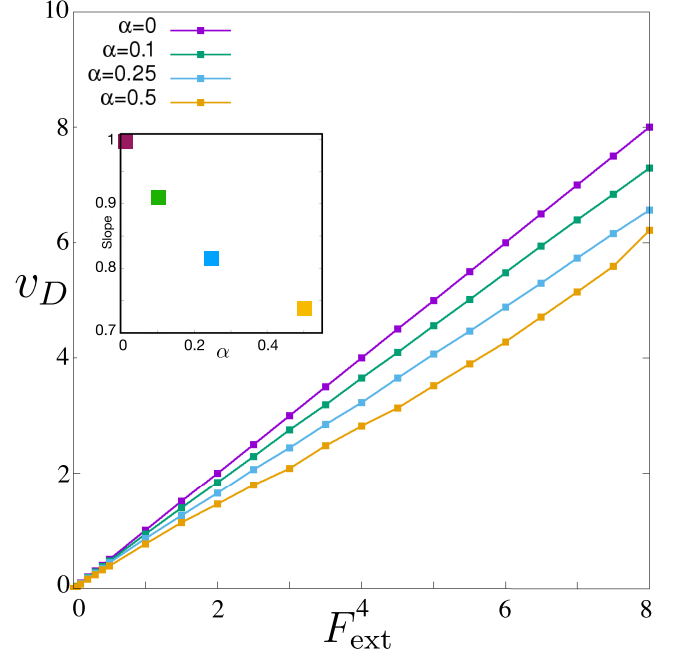

FIG. 4. Average drift velocity is plotted with different external drive F_{ext}. For every F_{ext} the drift along the drive is maximum when $\alpha = 0$. It reduces gradually with increasing α. In the inset it has been shown that the rate of the change of the drift velocity with respect to F_{ext} ($\sim \frac{dv_D}{dF_{ext}}$) decreases with the particle roughness α. Here the rate is estimated by the slope of the straight lines fitted with v_D vs. F_{ext} plot. The color code here represents various values of α.

Equating u_1 and u_2, we estimate $F_c \simeq \frac{V_0}{\sigma}(1 + \alpha)$, which shows F_c increases with α, which qualitatively matches with the result from simulation, as shown in Fig. 2.

Next, we consider a state of the system with $F_{ext} \to F_c'^-$ and $\alpha > 0$. In this parameter space, oppositely moving lanes are well developed and adjacent to each other in the system. Particles which are within a lane and far from the boundaries of the lane are facing less resistance from its neighbors because all of them are moving along the same direction. For these particles, the interparticle friction is quite small. Though for the particles which are at the lane boundaries (i.e., at the interface between two oppositely moving lanes) they are facing resistance from the oppositely moving particles. Therefore for them the interparticle friction is large. Hence the effective friction faced by the interfacial particles between two lanes are more in comparison to the particles which are well inside a lane. This makes the interfacial particles slower in comparison to the other particles of a lane. One can estimate the difference between the velocity of an interfacial particle and a particle well inside a lane as $u_3 \equiv \frac{\alpha F_{ext}}{\gamma(1+\alpha)}$, which is zero for smooth ($\alpha = 0$) particles, as expected. This is the velocity estimate at which an interface between two oppositely moving lanes recedes, leaving a gap between them. This gap will eventually filled up by the particles coming from both the oppositely moving lanes due to their $\hat{y}$ directional fluctuating motion caused by the interparticle repulsive interaction. This eventually breaks the lanes at high external drive such that the mixed, nonuniform, no-laned state reenters. One can estimate F_c' by equating u_3 with u_2 as $F_c' \simeq \frac{V_0}{\sigma}(\frac{1+\alpha}{\alpha})$. It shows that

for smooth particles (i.e., $\alpha \to 0$), $F'_c \to \infty$, which means we do not have the reentrance of the no-lane state. Thus one can estimate the difference between these two thresholds as $\Delta F = F'_c - F_c \simeq \frac{V_0}{\sigma}\left(\frac{1-\alpha^2}{\alpha}\right)$. Clearly, ΔF reduces as α increases which qualitatively agrees with the result from simulation, as depicted in Fig. 1. Though it is not the most accurate estimate of ΔF as it depends also on the choice of ϕ_c which is not considered here. Note that when the interparticle friction dominates over fluid friction, i.e., $\alpha > 1$, no lane can form and thus the aforementioned estimates of F_c and F'_c are not valid. In our analysis $0 \leqslant \alpha \leqslant 1$.

From the discussion above, it is evident that the interparticle friction causes the effective friction faced by a particle to be space dependent. This makes the density distribution nonuniform, particularly at high external forces. To test this computationally, below we consider a toy equation of motion for the particles where, instead considering the interparticle friction explicitly, we consider the effective friction $G > 0$ to be space-dependent. Considering a configuration of the system with well-developed lanes one may assign properties like $G(x, y) = G(x, y + l)$ and $G(x, l) < G(x, l/2)$ (where l is the typical lane-width) to the effective friction. The inequality ensures that the effective friction inside a lane is less than the friction faced by the particles at the interface between two oppositely moving lanes.

It is noteworthy that the properties assigned to $G(x, y)$ is relevant only when lanes are well developed in the system, i.e., when $F_c < F_{ext} < F'_c$. In general, for all F_{ext}, G can have complex dependence on position and relative velocity (relative to the neighbors) of a particle, deriving which is beyond the scope of the current paper. Instead we assume a functional form of G that maintains the aforementioned properties for all values of external drives. Though the strength of the periodic modulation of G is small enough such that it cannot disturb the lane formation until $F_{ext} \leqslant F'_c$. When $F_{ext} > F'_c$, we will see that the periodic modulation in G affects the lane structure and eventually the lane order decreases. This essentially indicates that in the presence of contact dissipation, the effective friction faced by a particle within a laned state can be spatially periodic and it can destabilise the lane structure beyond a certain threshold value of external drive F'_c.

We assume the following simple functional form of $G(x, y)$ as:

$$G(x, y) = \gamma[1 + a\sin^2(\pi y/l)], \tag{7}$$

where $a > 0$ is the amplitude of the periodic modulation of G varying in space between its minimum value at the middle of a lane at $y = nl$, given by $G_{min} = \gamma$ and its maximum value at the interface between two oppositely moving lanes, i.e., at $y = (n + 1/2)l$, which is given by $G_{max} = \gamma(1 + a)$ (where $n = 0, 1, 2, 3, \dots$). The equation of motion of the ith particle will be

$$\frac{d^2\mathbf{r}_i}{dt^2} = \mathbf{F}_i^p - \sum_j \nabla_i U \pm \mathbf{F}_{ext}, \tag{8}$$

where the effective friction (both from the fluid and from the neighboring particles in contact) faced by the particle is given by $\tilde{\mathbf{F}}_i^p = -G(x, y)\mathbf{v}_i$. We simulate the aforementioned model in the same parameter space as before and evaluate ϕ with
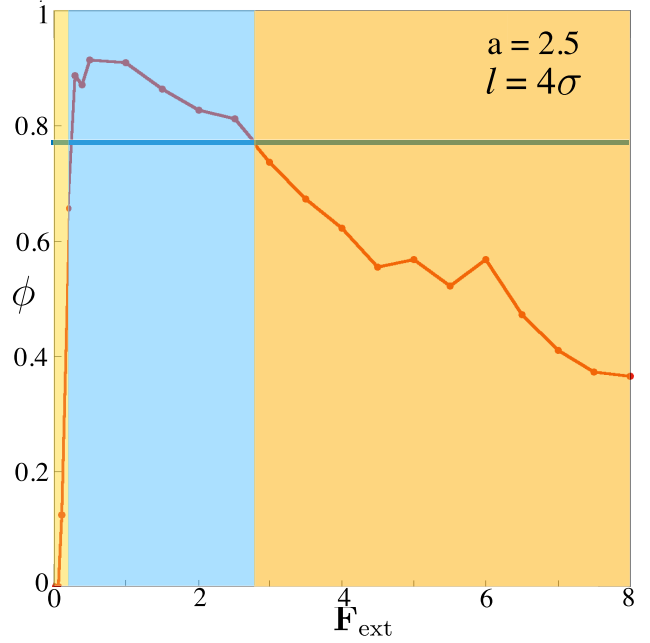

FIG. 5. Here we have plotted steady state ϕ with different external drive F_{ext} obtained by simulating Eq. (8). The blue horizontal straight line represents $\phi = \phi_c$. The blue rectangle represents the optimal values of F_{ext} for which $\phi > \phi_c$. The left boundary ($F = F_c$) of the rectangle represents the lower threshold of the external drive below which $\phi < \phi_c$. The right boundary ($F = F'_c$) of the rectangle represents the upper threshold of the external drive beyond which states with $\phi < \phi_c$ reenter.

different $|\mathbf{F}_{ext}|$ to obtain the Fig. 5. From the figure it is apparent that the model with space-dependent effective friction but without explicit interparticle friction provides qualitatively same results as obtained in Fig. 1. Initially, for very small F_{ext}, no lane was observed and $\phi < \phi_c$. Once $F_{ext} > F_c$ ($F_{ext} = F_c$ is the left boundary of the blue region in Fig. 5), lanes develop in steady states and hence $\phi > \phi_c$. As we increase F_{ext} further, once $F_{ext} > F'_c$ ($F_{ext} = F'_c$ is the right boundary of the blue region in Fig. 5), lanes start to break. Eventually ϕ becomes less than the threshold ϕ_c and no-lane state reenters. It is important to mention here that though there is qualitative similarity between the results from the aforementioned space-dependent effective friction model [Eq. (8)] and the model with explicit interparticle friction [Eq. (2)] in the context of the reentrant transition between laned and no-lane states, the rigorous relation between these two approaches is not yet established and it is beyond the scope of the current paper.

B. Effect of varying ρ on laning

All the data and the analysis above are at fixed average density (ρ) of the system. Here we will discuss what happens to the lanes when ρ is reduced, while maintaining the system as a 1:1 binary mixture as before. Note that it has already been discussed in Ref. [26] that for smooth colloidal particles, at high-enough ρ, jamming hinders lane formation. One may expect that the particle-scale roughness has strong impact on
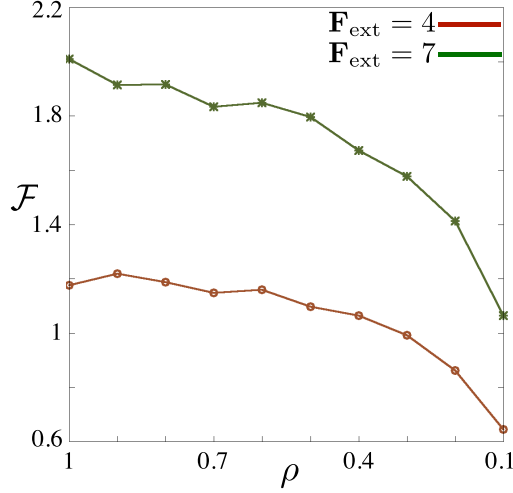
FIG. 6. Average interparticle friction force per particle $\mathcal{F}$ is plotted with average density ρ for two different external forces. Here $\alpha = 0.5$.

jamming and thereby on laning in the current context. It needs a separate study, which is beyond the scope of this article.

Here first we discuss that how the average interparticle friction per particle ($\mathcal{F}$) varies as we decrease ρ. It can be defined as $\mathcal{F} = \langle \frac{1}{N} \sum_i |\mathbf{F}_i^q| \rangle_\tau$ where τ indicates a steady-state time window within which the per particle interparticle frictional force is time averaged. In Fig. 6 we have shown that in nonequilibrium steady states, as ρ decreases, $\mathcal{F}$ decreases. This occurs because the number of frictional contacts among the particles, decreases as ρ is reduced.

Despite the decrease of the interparticle friction, the lane order drops with decreasing ρ. This is because the mean distance between any two particles ($\sim \frac{1}{\sqrt{\rho}}$) increases as ρ decreases. Consequently, between any two "a"-type particles, now it will be more likely to get a "b"-type particle and vice versa. Hence, at lower densities, irrespective of surface-roughness of the particles, the nonlaned mixed state becomes more favorable than the phase separated laned state. To illustrate this, in Fig. 7 we have plotted steady state ϕ with F_{ext} for different ρ. The plots are for two cases: [Fig. 7(a)] $\alpha = 0$ (smooth particles) and [Figs. 7(b) and 7(c)] $\alpha > 0$ (rough particles). In Figs. 7(a) and 7(b), initially ϕ increases with

F_{ext} but for higher values of F_{ext} it drops. The drop is much quicker for the systems with low ρ that favors the mixed state. The effect of lowering ρ on laning of rough particles becomes more clear when steady state ϕ is plotted with different ρ for three different F_{ext} in Fig. 7(c). As ρ decreases, ϕ reduces and vice versa, for all the three external drives. Above results also indicate that the lane formation in smooth particles ($\alpha = 0$) is a result of the interplay between F_{ext} and average interparticle repulsion per particle ($\equiv \mathcal{G} = \langle \frac{1}{N} \sum_i |\mathbf{F}_i^{sc}| \rangle_\tau$ where $\mathbf{F}_i^{sc} = -\sum_j \nabla_i U$). The interplay can be quantified by the ratio $\mathcal{R} = \frac{\mathcal{G}}{F_{ext}}$, the steady-state value of which is plotted in Fig. 8, together with ϕ, for different F_{ext} and for two different densities: $\rho = 1$ and $\rho = 0.1$. Initially (i.e., for small values of F_{ext}), for both the densities, $\mathcal{R}$ decreases with increasing F_{ext}. As F_{ext} increases further, $\mathcal{R}$ continues to decrease to reach a minima and then it increases with increasing F_{ext}. Finally, it saturates, forming a dip surrounding the minima. The dip indicates the competition between F_{ext} and $\mathcal{G}$. A balance between the interparticle screened-Coulombic repulsion and the external drive is established by the competition, leading toward lanes in the system. Therefore, for both the densities, ϕ becomes considerably high within the range of F_{ext} corresponding to the dip. Though, with increasing F_{ext} beyond the range, it starts to dominate over $\mathcal{G}$ and finally wins the competition. Consequently, $\mathcal{R}$ saturates and ϕ decreases for higher values of F_{ext}. According to Fig. 8, for $\rho = 1$, the competition between $\mathcal{G}$ and F_{ext} lasts for a longer range of F_{ext} than the case with $\rho = 0.1$. This makes the dip in $\mathcal{R}$ shallower and wider in case of $\rho = 1$, when plotted with F_{ext}. In the laned states with $\rho = 1$, as a result of the competition between $\mathcal{G}$ and F_{ext}, ϕ decreases slightly with increasing F_{ext}. Though it never goes below ϕ_c. On the other hand, when $\rho = 0.1$, ϕ continues to decrease with increasing F_{ext} and goes below ϕ_c.

Similarly, in the case of rough particles ($\alpha > 0$), it is important to understand the formation of lanes from a mixed state as a result of the interplay among three candidates: $\mathcal{G}$, $\mathcal{F}$, and F_{ext}, which is an impending task. Work along this direction is in progress.

VI. CONCLUSION

We consider a binary suspension of two types of particles in two dimensions, which move in opposite directions when subjected to a constant external drive. The particles are rough
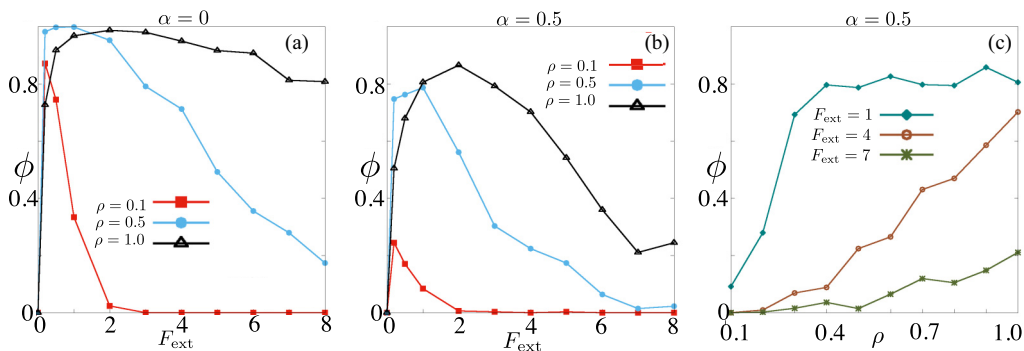

FIG. 7. In (a) (smooth particles) and (b) (rough particles), ϕ is plotted with F_{ext} for three different average densities ρ. In (c) (rough particles) ϕ is plotted with ρ for three different external drives. The figures essentially suggest that as ρ decreases, ϕ decreases, too.
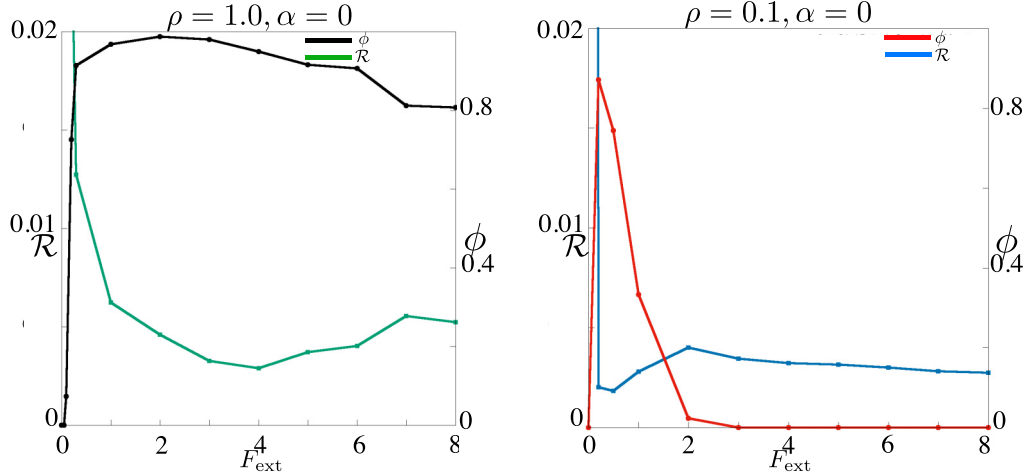
FIG. 8. The plots of $\mathcal{R}$ and ϕ with external drive F_{ext} in case of smooth particles ($\alpha = 0$) having average density $\rho = 1, 0.1$ are shown in (a) and (b), respectively,

and the density of the system is high enough such that the interparticle friction plays important role to the dynamics of the system. The thermal fluctuations are assumed to be insignificant in comparison to the other forces present in the system. We have shown that when the external drive goes beyond a threshold, the particles of different species segregate from the homogeneously mixed suspension to develop oppositely moving macroscopic lanes. The lane structure continues with increasing external drive up to a second threshold after which interparticle friction starts to dominate. Consequently the system cannot support the lanes anymore and we obtain a no-lane state. Note that for very low external drive, the system, being homogeneously mixed, does not support lanes. Therefore, with finite interparticle friction, we obtain the reentrance of no-lane state along the axis of increasing external drive.

There are few important related topics which deserve detailed, separate study. Though we leave them out from the current paper but we will mention them here briefly.

Transformation from no-lane state to laned state in binary colloidal systems (without interparticle contact dissipation) has significant finite-size effect [25]. It is important to study the finite-size effect here as well particularly for the reentrance of no-lane state at high external drive.

From the phase diagram in Fig. 3 it is apparent that as α increases F_c and F_c' come close to each other. Question is as follows: If we increase α further (which is not included in the current phase diagram), will there be a certain α for which F_c and F_c' merge to a single point in the phase diagram, beyond which no lane can be formed? If yes, then what will be the characteristics of that point in context of the phase transition.

Another important problem is the effect of varying differential average density ($|\rho_a - \rho_b|$) of the species on this reentrant laning transition. We have not discussed it in the current paper. Work along this direction is in progress.

Here thermal fluctuation associated with the temperature T of the suspension, is considered to be negligibly small in comparison to other forces as mentioned before. In other words, it is the limit where the Pèclet number (Pe) of the driven suspension is very large (i.e., Pe $\equiv \frac{F_{ext}\sigma}{K_B T} \to \infty$ where K_B is the Boltzmann constant). In the other extreme condition, where Pe $\to 0$ due to large T or vanishingly small F_{ext}, we do not expect lanes to be formed. Though we expect qualitatively similar behavior as detailed here, with sufficiently high F_{ext} and finite T, below a threshold temperature ($\equiv T^*$), such that the thermal forces are order of magnitude smaller than the other forces present in the system. It is an interesting, impending task to explore the reentrant laning transition for the suspension with varying T, particularly across T^*.

We believe our findings here are amenable to experiments with dense non-Brownian systems having significant frictional contacts among the particles (e.g., Ref. [34]).

[1] D. Helbing, L. Buzna, A. Johansson, and T. Werner, Transp. Sci. **39**, 1 (2005).

[2] D. Helbing and P. Molnar, in *Self-Organization Phenomena in Pedestrian Crowds*, edited by F. Schweitzer, Organization of Complex Structures: From Individual to Collective Dynamics (Gordon and Breach, London, 1997).

[3] I. D. Couzin and N. R. Franks, Proc. R. Soc. Lond. B **270**, 139 (2003).

[4] M. Yamao, H. Naoki, and S. Ishii, PLoS One **6**, e27950 (2011).

[5] F. Kogler and S. H. Klapp, Europhys. Lett. **110**, 10004 (2015).

[6] S. R. McCandlish, A. Baskaran, and M. F. Hagan, Soft Matter **8**, 2527 (2012).

[7] C. M. Surko, M. Leventhal, and A. Passner, Phys. Rev. Lett. **62**, 901 (1989).

[8] K. R. Sutterlin, A. Wysocki, A. V. Ivlev, C. Rath, H. M. Thomas, M. Rubin-Zuzic, W. J. Goedheer, V. E. Fortov, A. M. Lipaev, V. I. Molotkov, O. F. Petrov, G. E. Morfill, and H. Lowen, Phys. Rev. Lett. **102**, 085003 (2009).

[9] I. S. Aranson and L. S. Tsimring, Rev. Mod. Phys. **78**, 641 (2006).

[10] T. Börzsönyi, R. E. Ecke, and J. N. McElwaine, Phys. Rev. Lett. **103**, 178302 (2009).

[11] T. Mullin, Phys. Rev. Lett. **84**, 4741 (2000).

[12] M. E. Leunissen, C. G. Christova, A.-P. Hynninen, C. P. Royall, A. I. Campbell, A. Imhof, M. Dijkstra, R. Van Roij, and A. Van Blaaderen, Nature (London) **437**, 235 (2005).

[13] T. Vissers, A. Wysocki, M. Rex, H. Löwen, C. P. Royall, A. Imhof, and A. van Blaaderen, Soft Matter **7**, 2352 (2011).

[14] T. Vissers, A. van Blaaderen, and A. Imhof, Phys. Rev. Lett. **106**, 228303 (2011).

[15] A. Yethiraj, Soft Matter **3**, 1099 (2007).

[16] J. Dobnikar, A. Snezhko, and A. Yethiraj, Soft Matter **9**, 3693 (2013).

[17] J. Dzubiella, G. P. Hoffmann, and H. Löwen, Phys. Rev. E **65**, 021402 (2002).

[18] H. Löwen and J. Dzubiella, Faraday Discuss. **123**, 99 (2003).

[19] K. Klymko, P. L. Geissler, and S. Whitelam, Phys. Rev. E **94**, 022608 (2016).

[20] C. W. Wächtler, F. Kogler, and S. H. L. Klapp, Phys. Rev. E **94**, 052603 (2016).

[21] M. Rex and H. Löwen, Phys. Rev. E **75**, 051402 (2007).

[22] M. Rex and H. Löwen, Eur. Phys. J. E **26**, 143 (2008).

[23] M. Rex, Kolloidale Weiche Materie in äußeren Feldern: Theorie und Simulation, Ph.D. thesis (2008), https://docserv.uni-duesseldorf.de/servlets/DocumentServlet?id=7606.

[24] A. Poncet, O. Bénichou, V. Démery, and G. Oshanin, Phys. Rev. Lett. **118**, 118002 (2017).

[25] T. Glanz and H. Löwen, J. Phys.: Condens. Matter **24**, 464114 (2012).

[26] J. Chakrabarti, J. Dzubiella, and H. Löwen, Phys. Rev. E **70**, 012401 (2004).

[27] H. Perrin, C. Clavaud, M. Wyart, B. Metzger, and Y. Forterre, Phys. Rev. X **9**, 031027 (2019).

[28] R. Williamson, J. Phys. Chem. **35**, 354 (2002).

[29] C. Heussinger, Phys. Rev. E **88**, 050201(R) (2013).

[30] X. Cheng, J. H. McCoy, J. N. Israelachvili, and I. Cohen, Science **333**, 1276 (2011).

[31] H. Barnes, J. Rheol. **33**, 329 (1989).

[32] J. Mewis and N. J. Wagner, *Colloidal Suspension Rheology* (Cambridge University Press, Cambridge, UK, 2012).

[33] E. Brown and H. M. Jaeger, Phys. Rev. Lett. **103**, 086001 (2009).

[34] C.-P. Hsu, S. N. Ramakrishna, M. Zanini, N. D. Spencer, and L. Isa, Proc. Natl. Acad. Sci. USA **115**, 5117 (2018).

[35] L. C. Hsiao and S. Pradeep, Curr. Opin. Colloid Interface Sci. **43**, 94 (2019).

[36] R. A. Bagnold, Proc. R. Soc. Lond. A **225**, 49 (1954).

[37] A. Metzner and M. Whitlock, Trans. Soc. Rheol. **2**, 239 (1958).

[38] R. Hoffman, Trans. Soc. Rheol. **16**, 155 (1972).

[39] R. Hoffman, J. Colloid Interface Sci. **46**, 491 (1974).

[40] J. Bender and N. J. Wagner, J. Rheol. **40**, 899 (1996).

[41] W. J. Frith, P. d'Haene, R. Buscall, and J. Mewis, J. Rheol. **40**, 531 (1996).

[42] M. Fagan and C. Zukoski, J. Rheol. **41**, 373 (1997).

[43] G. P. Shrivastav, P. Chaudhuri, and J. Horbach, J. Rheol. **60**, 835 (2016).

[44] W. H. Boersma, J. Laven, and H. N. Stein, AIChE J. **36**, 321 (1990).

[45] P. d'Haene, J. Mewis, and G. Fuller, J. Colloid Interface Sci. **156**, 350 (1993).

[46] V. T. O'Brie and M. E. Mackay, Langmuir **16**, 7931 (2000).

[47] B. J. Maranzano and N. J. Wagner, J. Rheol. **45**, 1205 (2001).

[48] B. J. Maranzano and N. J. Wagner, J. Chem. Phys. **114**, 10514 (2001).

[49] D. Lootens, P. Hébraud, E. Lécolier, and H. Van Damme, Oil Gas Sci. Technol. **59**, 31 (2004).

[50] D. Lootens, H. van Damme, Y. Hémar, and P. Hébraud, Phys. Rev. Lett. **95**, 268302 (2005).

[51] R. J. Larsen, J.-W. Kim, C. F. Zukoski, and D. A. Weitz, Phys. Rev. E **81**, 011502 (2010).

[52] E. Bertrand, J. Bibette, and V. Schmitt, Phys. Rev. E **66**, 060401(R) (2002).

[53] E. Brown and H. M. Jaeger, J. Rheol. **56**, 875 (2012).

[54] A. Fall, A. Lemaitre, F. Bertrand, D. Bonn, and G. Ovarlez, Phys. Rev. Lett. **105**, 268303 (2010).

[55] A. Fall, F. Bertrand, G. Ovarlez, and D. Bonn, J. Rheol. **56**, 575 (2012).

[56] A. Lemaître, J.-N. Roux, and F. Chevoir, Rheol. Acta **48**, 925 (2009).

[57] M. E. Cates, J. P. Wittmer, J.-P. Bouchaud, and P. Claudin, Phys. Rev. Lett. **81**, 1841 (1998).

[58] A. Bérut, H. Chauvet, V. Legué, B. Moulia, O. Pouliquen, and Y. Forterre, Proc. Natl. Acad. Sci. USA **115**, 5123 (2018).

[59] N. Kumar, H. Soni, S. Ramaswamy, and A. Sood, Nat. Commun. **5**, 4688 (2014).

[60] G. Briand, M. Schindler, and O. Dauchot, Phys. Rev. Lett. **120**, 208001 (2018).

[61] D. J. Durian, Phys. Rev. Lett. **75**, 4780 (1995).

[62] E. Irani, P. Chaudhuri, and C. Heussinger, Phys. Rev. Fluids **4**, 074307 (2019).

[63] D. Vågberg, P. Olsson, and S. Teitel, Phys. Rev. Lett. **112**, 208303 (2014).

[64] F. Varnik, S. Mandal, V. Chikkadi, D. Denisov, P. Olsson, D. Vågberg, D. Raabe, and P. Schall, Phys. Rev. E **89**, 040301(R) (2014).

[65] A. Lemaître and C. Caroli, Phys. Rev. Lett. **103**, 065501 (2009).

[66] E. Irani, P. Chaudhuri, and C. Heussinger, Phys. Rev. Lett. **112**, 188303 (2014).

[67] P. Chaudhuri, V. Mansard, A. Colin, and L. Bocquet, Phys. Rev. Lett. **109**, 036001 (2012).

[68] C. S. O'Hern, A. J. Liu, and S. R. Nagel, Phys. Rev. Lett. **93**, 165702 (2004).

[69] J. C. Crocker and D. G. Grier, Phys. Rev. Lett. **73**, 352 (1994).

[70] J. K. Dhont, *An Introduction to Dynamics of Colloids* (Elsevier, Amsterdam, 1996).

[71] D. O. Riese, G. H. Wegdam, W. L. Vos, R. Sprik, D. Fenistein, J. H. H. Bongaerts, and G. Grübel, Phys. Rev. Lett. **85**, 5460 (2000).

[72] M. P. Allen and D. J. Tildesley, *Computer Simulation of Liquids* (Oxford University Press, Oxford, 2017).